

High-sensitivity study of laser-induced birefringence and dichroism in the ionization continuum of cesium

S. Cavalieri

*Dipartimento di Fisica, Università di Firenze and European Laboratory for Non-Linear Spectroscopy (LENL),
Largo Enrico Fermi 2, I-50125 Firenze, Italy*

M. Matera

Istituto di Elettronica Quantistica, Consiglio Nazionale delle Ricerche, Via Panciatichi 56/30, I-50127 Firenze, Italy

F. S. Pavone

European Laboratory for Non-Linear Spectroscopy (LENL), Largo Enrico Fermi 2, I-50125 Firenze, Italy

Jian Zhang, P. Lambropoulos, and T. Nakajima

Department of Physics, University of Southern California, Los Angeles, California 90089-0484;

Foundation for Research and Technology-Hellas, Institute of Electronic Structure & Laser,

P.O. Box 1527, Heraklion 71110, Crete, Greece;

and Department of Physics, University of Crete, Crete, Greece

(Received 14 September 1992)

We present an experimental study of laser-induced continuum structure in cesium, performed by observing the birefringence and dichroism induced in the atomic medium by a circularly polarized laser embedding the $8s^2S_{1/2}$ state into the ionization continuum. The optimization of the sensitivity for the detection of the polarization rotation has allowed a high-accuracy measurement of the resonance profile. A quantitative comparison with theoretical predictions, taking into account the hyperfine structure of atomic levels, shows a clear evidence of a line-broadening effect due to cesium resonant collisions.

PACS number(s): 32.80.Rm, 32.70.Jz, 32.80.Wr

I. INTRODUCTION

The study and uses of quantum-mechanical interference between transition amplitudes involving the atomic ionization continuum have attracted considerable interest in recent years, in a large part due to the availability of a variety of coherent tunable radiation sources (lasers). Interference phenomena within the atomic continuum have been studied for several decades now, especially in connection with the phenomenon of autoionization. The most widely known model for the simplest case of autoionization, namely one discrete state embedded in a continuum, was formulated by Fano [1], who derived a rather simple formal expression for the photoabsorption profile in terms of a single dimensionless parameter q , also referred to as the asymmetry parameter. The interference in that case is due to paths (channels) established by intra-atomic interactions such as configuration interaction, angular momentum recoupling, etc. What has given renewed impetus to the study of analogous phenomena induced by lasers is the possibility of controlling the interference through the judicious choice of the external radiation, creating thereby a seemingly unlimited variety of effects.

One interesting aspect of this variety is that one can also create interference in transitions between bound states as well, which may result in a number of effects such as population trapping [2] or the laser-induced transparency of an atomic medium to radiation nearly resonant with an atomic transition between two discrete

states one of which may be autoionizing, as reported recently by Boller, Imamoglu, and Harris [3]. It has also been argued that, at least within certain simplified models, population trapping may occur even when transitions through the continuum are involved [4] and particularly in the coupling of Rydberg levels through transition amplitudes via the continuum [5]. The common aspect among such laser-induced coherent phenomena involving the continuum is that, in contrast to its traditional role as a seat of irreversibility (decay), the continuum can now participate in processes leading back to bound states, even when the energy of the electron has been raised above the ionization threshold. Putting it in somewhat different terms, the presence of an amplitude that has a pole in the continuum does not necessarily imply only decay if an additional, appropriately chosen radiation source is also present.

A topic in this category that has received renewed attention recently is the so-called laser-induced continuum structure (LICS), first predicted by Heller and Popov in 1976 [6]. These authors have shown that a featureless continuum, such as, for instance, that of an alkali-metal atom not far from threshold, can be structured by a strong laser field embedding a low-lying bound state in the continuum, as shown in Fig. 1. The dressed atomic system, i.e., the combined atom-plus-laser system, probed by a weak radiation field of frequency ω_p , may exhibit an autoionizinglike resonance in the photoionization spectrum, usually referred to as LICS. One feature of the expected structure is the possibility of an asymmetric

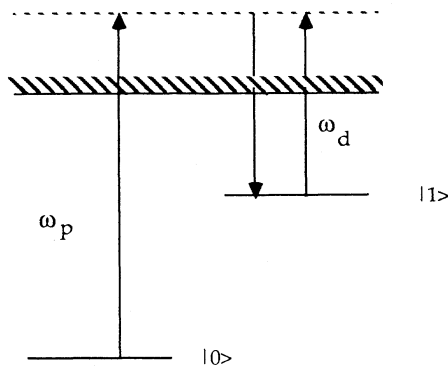


FIG. 1. Schematic diagram illustrating LICS. The strong laser field of frequency ω_d (dressing laser) couples the state $|1\rangle$ to the continuum states $|\epsilon\rangle$. The structure induced in the continuum is probed by the weak laser of frequency ω_p .

profile, similar to that of a Fano resonance, denoting quantum-mechanical interference between different transition pathways: (a) photoionization from state $|0\rangle$, induced by the probe laser and (b) photoionization from state $|1\rangle$, induced by the dressing laser, following the two-photon transition $|0\rangle \rightarrow |1\rangle$. Moreover, the position and width of the resonance are dependent on the frequency and intensity of the dressing field, respectively.

Besides the photoionization spectrum, the LICS is expected to affect a number of other processes in the continuum, through a modification of the atomic susceptibility. In fact, the first evidence of LICS was provided in 1981 by the measurement of the birefringence and dichroism induced by the dressing laser on the atomic medium [7]. The polarization rotation effects underlying this technique were previously studied by Liao and Bjorklund [8] for a two-photon transition of sodium: the linear polarization of a laser field of frequency ω_1 (signal laser) was found to be rotated by a circularly polarized laser field of frequency ω_2 (control laser), when $\omega_1 + \omega_2$ was tuned near the $3s^2S_{1/2} - 5s^2S_{1/2}$ two-photon transition frequency. The polarization rotation effect is a result of the selection rules for a two-photon transition: in the case of an S to S transition of an alkali-metal atom, for the absorption to be allowed the photons must have opposite senses of circular polarization. Hence a right circularly polarized laser will affect only the left circular component of a linearly polarized signal field. The absorptive and dispersive parts of the two-photon susceptibility will cause respectively a light-induced birefringence and dichroism, giving rise to an elliptical polarization. The application of this technique (characterized by the high sensitivity typical of polarization spectroscopy) to the LICS is straightforward, since this process involves a two-photon coupling between the ground state $|0\rangle$ and the excited state $|1\rangle$ with an intermediate state in the continuum.

In contrast to the extensive theoretical work reported in literature [9], only few experimental studies of LICS have been reported. LICS evidence has been reported in

the enhancement of third-harmonic generation in sodium [10], although a subsequent experiment [11] under somewhat different conditions responsible for the outcome [12] has not confirmed the effect. An observation of LICS in the multiphoton ionization spectrum of xenon reported by Hutchinson and Ness [13] was not suitable for a comparison with theory [14], owing to the pronounced background. Recently, the observation of LICS in the single-photon ionization spectrum of sodium has been reported [15,16]. The study of LICS in photoionization experiments is made more difficult by the presence of transition pathways involving intermediate bound states, as shown in the experiments by Feldmann *et al.* [17], where a careful investigation of multiphoton ionization of sodium in the presence of two laser fields was carried out.

The review of existing experimental studies of LICS allows us to draw the following conclusions: (i) some experimental results are not fully consistent with each other or with theoretical predictions and (ii) difficulties in observing LICS are in contrast with simple theoretical models predicting a conspicuous effect. A deeper experimental study with an accuracy suitable for relating the observed line shape to the relevant atomic parameters and to the theoretical description of the interaction dynamics is therefore needed. In fact, it is not yet clear whether the reason for some of the observed discrepancies lies in the actual experimental conditions, which are not fully considered in theoretical models, or in the basic assumptions of the description of the dynamics. It is worth noting here that the LICS is critically dependent on atomic parameters, such as photoionization rates from excited states or energy shift terms, which are presently available mostly from calculations.

In this context, it is of great importance to perform experiments both in the strong- and weak-field regimes, with reference to the dressing laser intensity. In fact, at increasing intensity, the width of the structure becomes dependent on the photoionization rate from the excited state while the resonance frequency is shifted by a dynamic Stark effect. As a result, the line shape becomes dependent on the temporal and spatial intensity distribution of the dressing laser, which is very difficult to control for high-intensity pulsed lasers. These drawbacks are not expected to affect a weak-field measurement, making attractive the availability of a very sensitive technique based on the measurement of the light-induced birefringence and dichroism.

In this paper, we present a high-accuracy study of LICS in cesium carried out by using the highly sensitive polarization technique described above. A careful adjustment of the setup allowed an improvement of sensitivity for the detection of polarization rotation by two orders of magnitude as compared to that of Ref. [7]. The main purpose of the study is a quantitative interpretation of the line shape, taking into account the laser bandwidths and the hyperfine structure of atomic levels, which were not previously considered. The results provide a complementary information to that given by photoionization experiments. Finally, measurements performed at different cesium densities show a clear evidence of line-broadening effects due to resonant collisions.

II. THEORY

The physical system studied is illustrated in the diagram of Fig. 2. We consider a ground-state cesium atom interacting with a strong laser field of frequency ω_d (dressing laser), which may couple a number of bound states to other bound states or to the continuum. In particular the structure induced in the continuum (LICS) by the coupling to the $8s\ ^2S_{1/2}$ state can be probed by irradiating the atom with a second weak laser field of frequency

$$\omega_p \approx \omega_d + \frac{E(8s\ ^2S_{1/2}) - E(6s\ ^2S_{1/2})}{\hbar}. \quad (1)$$

The LICS will affect the photoionization rate, giving rise to a Fano-type resonance, whose profile is dependent on atomic parameters and on laser intensities. Moreover, in the proximity of the resonance, the atomic medium may exhibit birefringent and dichroic behavior. In fact, according to the selection rules for two-photon transitions, the $6s\ ^2S_{1/2}$ and $8s\ ^2S_{1/2}$ states, for a σ^- polarization of the dressing laser, can be coupled to each other only by the σ^+ component of the probe laser, through the intermediate $m = +\frac{1}{2}, +\frac{3}{2}$ continuum states. As a consequence, if the probe laser is assumed linearly polarized, the σ^+ and σ^- components will undergo, for frequencies close to the two-photon resonance, different absorption and phase shift, causing the polarization to be rotated and to become elliptical. The LICS can therefore be studied by analyzing the polarization of the probe beam emerging from the atomic medium. Let θ_0 be the angle by which the analyzing polarizer is rotated from the position perpendicular to the polarization of the probe beam incident on the atomic medium. As a result of the combined effect of absorption and dispersion, the transmittance of the polarizer can be written as

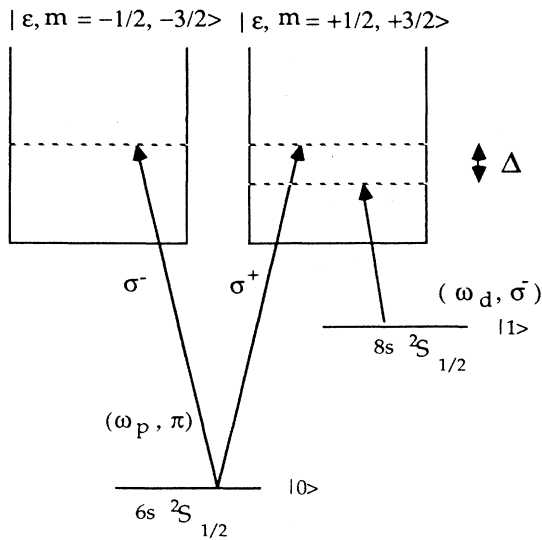


FIG. 2. Diagram of energy levels and transitions of cesium relevant to the LICS process. (ω_d, σ^-) and (ω_p, π) denote frequency and polarization of the dressing and probe laser, respectively.

$$T(\Delta) = [\theta_0 + \theta(\Delta)]^2 + A^2(\Delta), \quad (2)$$

where $\theta(\Delta)$ and $A(\Delta)$ are, respectively, polarization rotation and ellipticity, induced by the dressing laser, dependent on the detuning from the two-photon resonance:

$$\Delta = \omega_p - \omega_d - \frac{E(8s\ ^2S_{1/2}) - E(6s\ ^2S_{1/2})}{\hbar}. \quad (3)$$

For an interaction length L we have then

$$\theta = \frac{\pi\omega_p L}{c} \operatorname{Re} \left[\chi^+(\omega_p) - \chi^-(\omega_p) \right], \quad (4)$$

$$A = \frac{\pi\omega_p L}{c} \operatorname{Im} \left[\chi^+(\omega_p) - \chi^-(\omega_p) \right],$$

where $\chi^\pm(\omega_p)$ is the atomic susceptibility for the σ^\pm component of the probe laser, related to the density matrix $\hat{\rho}$ and the dipole moment \hat{d} by the general equation

$$\chi(\omega) = \frac{\operatorname{Tr}(\hat{d}\hat{\rho})}{E}, \quad (5)$$

where E denotes the electric-field amplitude at the frequency ω propagating in the medium. An explicit expression of (4) can be found by solving the equations of motion for the density matrix, involving bound as well as continuum states. The use of a Markovian approximation, allowing the elimination of the elements corresponding to bound- to free-state transitions, leads to a reduced set of equations for the slowly varying density matrix:

$$\begin{aligned} \frac{\partial}{\partial t} \sigma_{00} &= -\Gamma_{0\epsilon} \sigma_{00} - \operatorname{Im}[\sigma_{01} \Gamma_{01}(q+i)], \\ \frac{\partial}{\partial t} \sigma_{11} &= -\Gamma_{1\epsilon} \sigma_{11} + \operatorname{Im}[\sigma_{01} \Gamma_{01}(q-i)], \end{aligned} \quad (6)$$

$$\left[\frac{\partial}{\partial t} + i\Delta + \Gamma \right] \sigma_{01} = -i \frac{\Gamma_{01}}{2} [(q-i)\sigma_{11} - (q+i)\sigma_{00}],$$

where

$$\sigma_{ii} = \rho_{ii}, \quad i=0,1; \quad \sigma_{01} = \rho_{01} e^{i(\omega_p - \omega_d)t}.$$

In Eq. (6) we have neglected multiphoton processes as well as level shifts induced by the dressing laser, owing to the relatively low-intensity conditions of the experiment. In fact, the high sensitivity of the polarization technique allows an unfocused configuration to be used. $\Gamma_{0\epsilon}$ and $\Gamma_{1\epsilon}$ are the photoionization rates of states $|0\rangle$ and $|1\rangle$, respectively, related to the cross sections and laser intensities by

$$\Gamma_{0\epsilon} = \frac{\sigma_{0\epsilon}}{\hbar\omega_p} I_p, \quad \Gamma_{1\epsilon} = \frac{\sigma_{1\epsilon}}{\hbar\omega_d} I_d, \quad \Gamma_{01} = \sqrt{\Gamma_{0\epsilon} \Gamma_{1\epsilon}}, \quad (7)$$

$\sigma_{0\epsilon}$ and $\sigma_{1\epsilon}$ being the ionization cross sections from the states $|0\rangle$ and $|1\rangle$ due to the laser field at frequency ω_p and ω_d , respectively. Moreover, in Eq. (6) the effect of a finite bandwidth of the laser fields has been included, according to the phase-diffusion model. From the theory of multiplicative stochastic processes [18], the average of the density matrix over the distribution of the phase fluctuations, considered as undergoing a Markovian process,

is found to satisfy Eq. (6) with a damping term for the coherence given by

$$\Gamma = \frac{\delta\omega_p + \delta\omega_d + \Gamma_{0\epsilon} + \Gamma_{1\epsilon}}{2} \quad (8)$$

with $\delta\omega_p$ and $\delta\omega_d$ bandwidths [full width at half maximum (FWHM)] of the probe and dressing laser, respectively [19]. Finally, q is an atomic parameter playing the same role as the Fano parameter in the autoionization (for a detailed definition see Ref. [20]). Since $I_p \ll I_d$ we can assume $\Gamma_{0\epsilon} \ll \Gamma_{1\epsilon}$. In the case of $\tau\Gamma_{0\epsilon} \ll 1$ and $\tau\Gamma_{1\epsilon} > 1$ (τ is the interaction time, determined by the duration of the laser pulses) an analytical solution of (6) can be easily found by perturbative methods. Notice that, if the condition

$$\Gamma_{1\epsilon} \ll \delta\omega_p + \delta\omega_d \quad (9)$$

is satisfied, the shape of the resonance will not be affected by the intensity of the dressing laser. Under the weak-field condition defined by (9) the polarization rotation θ and ellipticity A can be expressed in terms of the coherence σ_{01} as

$$\theta \propto \text{Re}[\Gamma_{01}(q+i)\sigma_{01}], \quad (10)$$

$$A \propto \text{Im}[\Gamma_{01}(q+i)\sigma_{01}].$$

A perturbative solution of Eq. (6) (based on the condition $\sigma_{00} \approx 1$ and $\sigma_{11} \ll 1$) to first order in $\Gamma_{0\epsilon}$ provides

$$\sigma_{01} \approx \frac{i}{2} \frac{\Gamma_{01}(q+i)}{i\Delta + \Gamma} \quad (11)$$

from which we obtain

$$\theta(x) \propto \left[\frac{\Gamma_{1\epsilon}}{2\Gamma} \right] \frac{(q^2-1)x - 2q}{1+x^2}, \quad (12)$$

$$A(x) \propto \left[\frac{\Gamma_{1\epsilon}}{2\Gamma} \right] \frac{(q^2-1) + 2qx}{1+x^2},$$

where x is the detuning normalized to the off-diagonal relaxation Γ defined by $x = \Delta/\Gamma \approx 2\Delta/(\delta\omega_p + \delta\omega_d)$.

From (12) it is evident that the study of the LICS by

the resonant behavior of the birefringence and dichroism of the atomic medium allows a “zero” measurement. In fact, for $x \gg 1$, $\theta(x)$ and $A(x)$ vanish, in contrast to the photoionization which, far from resonance, reduces to a background.

A single measurement of the spectral transmittance of the analyzing polarizer to the probe laser beam can only provide a combined information on the birefringent and dichroic effect of the structure induced in the continuum by the dressing field. In fact, from Eq. (2) for $\theta_0=0$, we get

$$T(x,0) = \theta^2(x) + A^2(x) \propto \frac{(q^2+1)^2}{1+x^2}, \quad (13)$$

which is a Lorentzian profile with a width mainly determined by the laser bandwidths. Information on the birefringence alone can be obtained from the difference between two measurements of spectral transmittance, corresponding to opposite polarizer angles $+\theta_0$ and $-\theta_0$:

$$T(x, +\theta_0) - T(x, -\theta_0) = 4\theta_0(x)\theta_0$$

$$\propto D(x) = \frac{(q^2-1)x - 2q}{1+x^2}. \quad (14)$$

The resonance profile described by $D(x)$ exhibits a degree of asymmetry dependent on the value of the q parameter, making an accurate measurement of great interest not only for a test of the interaction dynamics, as is described by theoretical models of LICS, but also for an experimental determination of this atomic parameter.

For further comparison between experimental results and theory, besides the resonance profile, it is of great importance to evaluate the absolute polarization rotation angle which, for the system of our interest, combining Eqs. (4), (5), and (11) can be written as

$$\theta(x) = \frac{NI_d\sigma_{8s}\sigma_{6s}}{4\hbar\omega_d\Gamma} LD(x), \quad (15)$$

where N is the atomic density and L the length of the interaction region.

For an accurate study of the LICS line shape, particular attention must be paid to the hyperfine structure of the atomic levels involved in the process, schematically shown in Fig. 3. In effect, in cell experiments both sub-

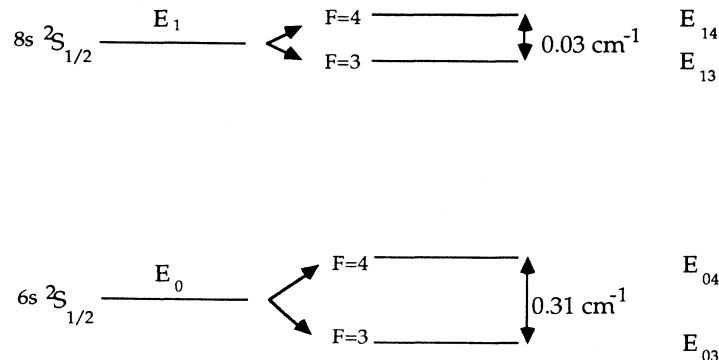


FIG. 3. Hyperfine structure of the ground- and excited-state cesium levels involved in the LICS process. Level separations are not to scale. The nuclear spin of the cesium atom is $I = \frac{7}{2}$.

levels of the ground state are populated. Moreover, the finite bandwidth of laser sources suitable for the experiment overlaps all sublevels of the doublet. In general, a coherent treatment of the interaction in terms of the complete density matrix of the system in the hyperfine scheme would be desirable. This, however, is not necessary in our case because the duration of the pulse is sufficiently long and the intensity sufficiently low for a simple treatment in terms of a rate equation to be valid. Moreover, after some angular momentum algebra one can show that the ionization width of the hyperfine levels involved are all the same, due to the fact that the states involved are S states. Assuming thus a simple rate model and the same two-photon coupling Γ_{01} between every sublevel of the ground state and every sublevel of the excited state, we can write for $D(x)$ and $T(x,0)$ the expressions:

$$D(x) = \sum_{i,j=3}^4 \frac{(q^2-1)x_{ij} - 2q}{1+x_{ij}^2}, \quad (16a)$$

$$T(x,0) = \left[\sum_{i,j=3}^4 \frac{(q^2-1)x_{ij} - 2q}{1+x_{ij}^2} \right]^2 + \left[\sum_{i,j=3}^4 \frac{(q^2-1) + 2qx_{ij}}{1+x_{ij}^2} \right]^2, \quad (16b)$$

where $x_{ij} = \Delta_{ij}/\Gamma$ and $\Delta_{ij} = \omega_p - \omega_d - (E_{1i} - E_{0j})/\hbar$, with E_{0i} and E_{1j} energy levels, defined as shown in Fig. 3. The result (16) is valid assuming the same population in each ground-state sublevel, which is the case in our experiment.

In concluding this section, we wish to emphasize the main properties of the polarization technique, favorable to a high-accuracy study of the LICS process.

(i) Due to the extinction ratio of commercial polarizers, the measurement of the laser-induced birefringence is characterized by the high sensitivity and accuracy typical of a "zero" measurement.

(ii) As a consequence of the sensitivity of the technique, a study of the LICS in the weak-field regime, i.e., with an unfocused geometry, is possible.

(iii) Level-shift terms, which introduce additional complications, are negligible.

(iv) The shape of the resonance is not dependent on the laser intensity, making an average on the temporal and spatial field distribution in the interaction region unnecessary.

III. EXPERIMENTAL SETUP

The experimental setup is schematically shown in Fig. 4. The laser system consists of a dye laser (Quantel model TDL-50) pumped by the second harmonic of a Q-switched pulsed Nd:YAG laser (where YAG denotes yttrium aluminum garnet) (Quantel model YG-581-C). The pump laser, including an injection-seeded Gaussian oscillator and a 9-mm-diam amplifier, provides single-mode smooth pulses at $\lambda = 1064$ nm with 1-J energy, 6-ns duration (FWHM), and 0.003-cm^{-1} bandwidth at 10 pulses/sec. A fraction of the Nd:YAG laser energy

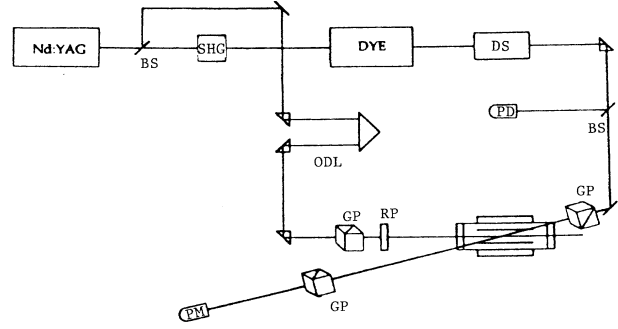


FIG. 4. Schematic diagram of the experimental apparatus: SHG, second-harmonic generator; DS, optical doubling system; PD, normalization photodiode; BS, beam splitter; ODL, optical delay line; RP, $\lambda/4$ retarding plate; GP, Glan Polarizer; PM, photomultiplier.

(≈ 100 mJ) reflected by a beam splitter is used as dressing laser. Efficient second-harmonic generation in a temperature-stabilized potassium dihydrogen phosphate (KDP) crystal provides high-intensity pulses at $\lambda = 532$ nm, suitable for dye pumping. The dye laser, consisting of an oscillator, followed by two amplifier stages, operated with rhodamine 610, provides linearly polarized radiation, tunable around 593 nm, with ≈ 50 -mJ energy. The bandwidth of the dye laser, whose oscillator is based on a near-grazing grating configuration, with a four-prism beam expander, is $\approx 0.1\text{ cm}^{-1}$. Owing to mode beating in the oscillator cavity, the temporal profile of the dye emission exhibits a modulation with ≈ 2 -ns period and $\approx 30\%$ depth. An absolute calibration of the frequency of the dye emission has given the laser frequency within $\pm 0.2\text{ cm}^{-1}$. The second-harmonic of the dye laser at $\lambda = 296.6$ nm is used to probe the structure induced in the cesium atom by the dressing laser, embedding the state $8s^2S_{1/2}$ in the continuum. Frequency conversion is achieved in a KDP crystal driven by a closed loop system, allowing tracking during frequency scans. The second-harmonic and the fundamental fields are separated by a Pellin-Broca prism. The probe laser pulses are characterized by a maximum energy of ≈ 1 mJ, a bandwidth of $\approx 0.2\text{ cm}^{-1}$, and a duration of ≈ 4 ns. The resolution and resettability of the frequency scanning system of the dye laser are better than the emission bandwidth. The ir beam, after passing through a variable optical delay line for optimum timing, is circularly polarized by a $\lambda/4$ retarding plate following a Glan polarizer (Optics for Research, Model PHU 15), with a residual ellipticity $\approx 90\%$. The required intensity of the dressing field ($\approx 10^8\text{ W/cm}^2$) in an unfocused configuration is reached by a telescope with magnification $\frac{1}{3}$, not shown in the figure, reducing the diameter of the beam to ≈ 2.5 mm, approximately equal to that of the uv beam. The probe and dressing laser beams overlap in the center of the interaction region for a length ≈ 5 cm crossing at an angle of $\approx 3^\circ$ in counterpropagating geometry. Cesium is evaporated in a conventional stainless-steel heat pipe with water-cooled ends. Argon buffer gas at a pressure ≈ 50 mbar is used to prevent vapor deposition on the fused silica windows.

The uv laser beam, linearly polarized by a Glan prism after interacting with the atomic medium dressed by the ir field, is analyzed by a second Glan prism. The residual uv field transmitted by the crossed polarizers is detected by a solar blind photomultiplier (EMI Model 9412) and measured by a synchronous integrator (SRS Model SR 250) with a gate width ≈ 100 ns, interfaced to an IBM XT-286 personal computer for data acquisition and processing.

Since the sensitivity for the detection of the polarization rotation induced by the LICS depends on the extinction ratio of the crossed polarizers, we have performed a careful measurement of the transmission curve for the uv field versus the rotation angle θ_0 of the analyzing polarizer from the position of minimum transmittance. An accurate positioning of the analyzing polarizer was allowed by measuring the deviation angle of a He-Ne laser beam reflected by a mirror attached to the body of the polarizer. The depolarization of the beam due to the transmission through the cell was minimized by properly rotating and stressing the windows (fused silica: Suprasil I). By fitting the experimental data taken at $\lambda = 296.6$ nm with the theoretical transmittance, the extinction ratio for the conditions of the experiment was found to be 2×10^{-7} , allowing a sensitivity of about 0.1 mrad. This result could not be obtained by using a collinear geometry, where a partially reflecting element is needed to direct the uv beam emerging from the heat pipe towards the analyzing polarizer. In fact the depolarization introduced by this element was found to make the extinction ratio worse by at least one order of magnitude.

While the Nd:YAG emission, used as dressing field, has energy fluctuations from pulse to pulse $\approx 1-2\%$, the second harmonic of the dye emission, used as probe field, has fluctuations up to 20–30%. The linear dependence of the transmitted field on the probe field intensity [Eq. (2)] suggests pulse by pulse normalization of the output signal in order to reduce these fluctuations to $\approx 10\%$. The normalization signal was provided by a photodiode detecting the field reflected by a beam splitter on the uv beam path. The normalized signal is then averaged over ≈ 100 laser pulses.

IV. RESULTS AND DISCUSSION

In Fig. 5 we have reported the dispersive profile of the LICS measured through the spectral transmittance of the crossed polarizers. The ellipticity due to the laser-induced dichroism has been eliminated by performing the difference between the spectral transmittances $T(x, +\theta_0)$ and $T(x, -\theta_0)$ measured for $\theta_0 = 0.60 \pm 0.05$ mrad. From the measurement of $T(x, +\theta_0)$ and the values of the extinction ratio of the polarizers and θ_0 , a maximum rotation angle $\theta_{\max} \approx 1$ mrad is evaluated. The dressing and probe laser intensities were $I_d = 200$ MW/cm² (pulse energy $E_d = 60$ mJ) and $I_p = 100$ kW/cm² (pulse energy $E_p = 20$ μ J), respectively. The heat pipe was operated at the temperature $T = 320^\circ\text{C}$ with 30 mbar of argon as the buffer gas, providing a cesium numerical density $\approx 4.8 \times 10^{16}$ atoms/cm³. In these conditions, a polarization rotation of ≈ 0.1 mrad, which is a factor 5 better

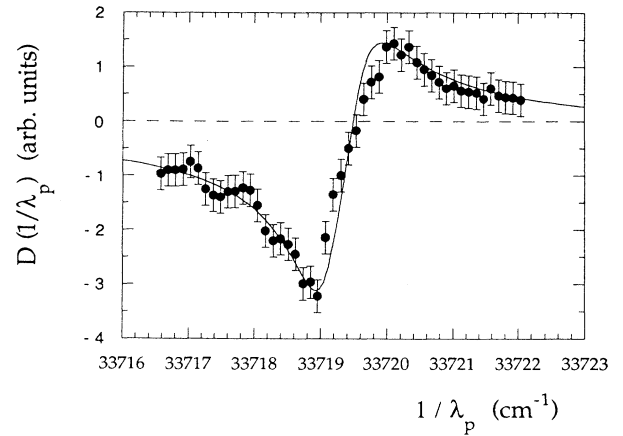


FIG. 5. Dispersive profile of LICS vs the inverse of the air wavelength of the probe laser. Heat-pipe temperature $T = 320^\circ\text{C}$. The solid line is a best fit of (16a) giving $\Gamma = 0.41 \pm 0.07$ cm⁻¹.

than the previously reported minimum detectable rotation [7], was found to produce a signal variation of $\approx 20\%$ in the spectral transmittance $T(x, +\theta_0)$, with an improvement of about two orders of magnitude on what can be inferred from Ref. [7]. The solid line in Fig. 5 is a best fit of the theoretical profile (16a) corresponding to an asymmetry parameter $q = 6.4$, resulting from our atomic structure calculations based on single-channel quantum-defect theory. The photoionization cross sections of the $8s^2S_{1/2}$ and $6sS_{1/2}$ cesium states at the wavelength of the probe and dressing laser, respectively, have been assumed as $\sigma_{6s} = 1.1 \times 10^{-19}$ cm² (experimental data in Ref. [21]) and $\sigma_{8s} = 8.7 \times 10^{-19}$ cm² (our numerical calculation). The corresponding photoionization rates at the intensities of the measurement are $\Gamma_{0e}/2\pi c = 8.7 \times 10^{-13} I_p$ cm⁻¹ (I_p in W/cm²) $\approx 8.7 \times 10^{-8}$ cm⁻¹ and $\Gamma_{1e}/2\pi c = 2.5 \times 10^{-11} I_d$ cm⁻¹ (I_d in W/cm²) $\approx 5.0 \times 10^{-3}$ cm⁻¹, satisfying the conditions of validity for the perturbative solution (16). In our experimental conditions, we also have $\Gamma_{0e} \ll \Gamma_{1e}$ and $\Gamma_{1e} \ll \delta\omega_p + \delta\omega_d \approx \delta\omega_p$ so that the expected width of the resonance is $2\Gamma/2\pi c \approx \delta\omega_p/2\pi c \approx 0.2$ cm⁻¹.

By assuming as free parameters, besides a normalization factor for the amplitude scale, the coherence damping rate Γ , the best fit provides $\Gamma/2\pi c = 0.41 \pm 0.07$ cm⁻¹. The good agreement between theoretical and experimental resonance profiles provides then a check for the calculated q parameter. However, the resonance width resulting from the fit is larger than expected (0.8 cm⁻¹ in comparison to 0.2 cm⁻¹). For comparison we have also measured the spectral transmittance for $\theta_0 = 0$, reported in Fig. 6 with the best fit of the theoretical profile (16b), providing $\Gamma/2\pi c = 0.40 \pm 0.04$ cm⁻¹. The measurements seem therefore to definitively indicate the presence of an additional broadening mechanism not included in Eq. (8). We have then investigated the dependence of the spectral transmittance $T(x, 0)$, which is more easily measurable, on the experimental conditions. No variation of the shape has been observed when we vary the laser intensities in the ranges $2 \times 10^4 - 2 \times 10^5$

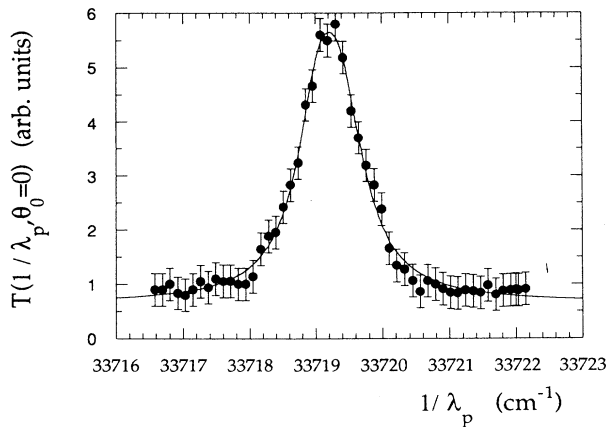


FIG. 6. Spectral transmittance measured for $\theta_0=0$. Heat-pipe temperature $T=320^\circ\text{C}$. The solid line is a best fit of (16b) giving $\Gamma=0.40\pm 0.04\text{ cm}^{-1}$.

W/cm^2 for I_p and $4\times 10^7\text{--}2\times 10^8\text{ W}/\text{cm}^2$ for I_d . Moreover, the profile was found unaffected by the buffer-gas pressure in the range 20–200 mbar. On the contrary, measurements performed at different cesium densities exhibit different widths. In Figs. 7(a) and 7(b) we have reported the spectra performed, respectively, at $T=380^\circ\text{C}$, corresponding to a cesium density $1.6\times 10^{17}\text{ atoms}/\text{cm}^3$, and at $T=430^\circ\text{C}$, corresponding to a cesium density $3.9\times 10^{17}\text{ atoms}/\text{cm}^3$. The best fits plotted in the figures provided for Γ the values $\Gamma/2\pi c=0.8\pm 0.1\text{ cm}^{-1}$ ($T=380^\circ\text{C}$) and $\Gamma/2\pi c=1.1\pm 0.2\text{ cm}^{-1}$ ($T=430^\circ\text{C}$), showing clear evidence of a broadening effect due to cesium resonant collisions.

Finally we wish to compare the maximum observed polarization rotation with the theoretical value given by (15). The effect of the collisional broadening on the polarization rotation is taken into account by simply assuming for Γ the value given by the best fit of the experimental spectrum. For the conditions of the measurement shown in Fig. 5, with $\Gamma/2\pi c=0.4\text{ cm}^{-1}$, we get from (15) $\theta_{\text{max}}\approx 2\text{ mrad}$, which has to be compared to the experimental value $\theta_{\text{max}}\approx 1\text{ mrad}$. Note that with the polarization technique used here, collisions may cause population transfer among magnetic sublevels, thereby reducing the measured polarization rotation. Even considering the moderate accuracy of the determination of some relevant atomic or experimental parameters, this result provides on the LICS process additional information to that given by the line-shape analysis: in the conditions of the experiment, the effect induced by the dressing laser is found to be quantitatively consistent with the theoretical predictions.

In conclusion, laser-induced continuum structure in atomic cesium vapor has been studied by observing two-photon polarization rotation effects. A careful optimization of the interaction conditions and of the sensitivity of the apparatus for the detection of polarization rotation

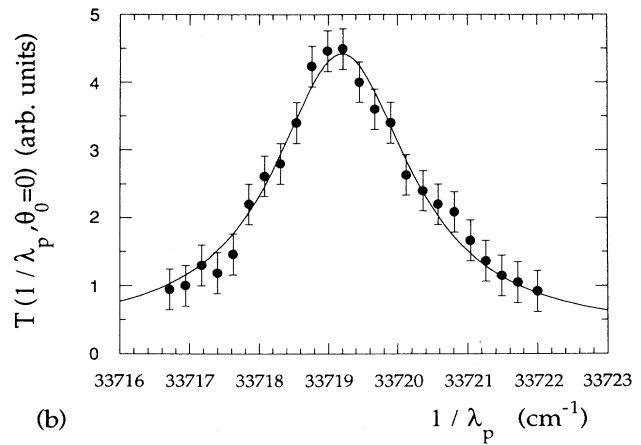
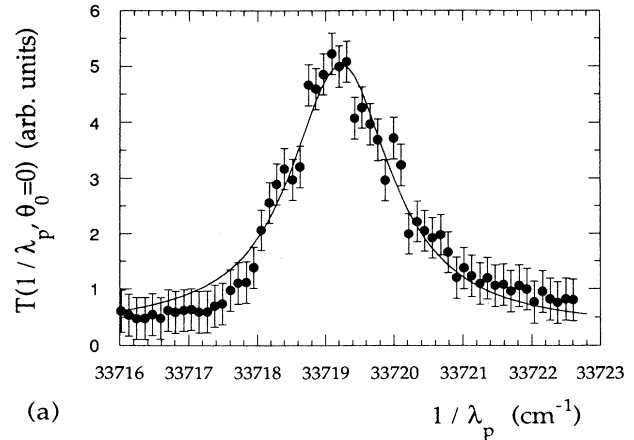


FIG. 7. (a) Spectral transmittance measured for $\theta_0=0$. Heat-pipe temperature $T=380^\circ\text{C}$. The solid line is a best fit of (16b) giving $\Gamma=0.8\pm 0.1\text{ cm}^{-1}$. (b) Spectral transmittance measured for $\theta_0=0$. Heat-pipe temperature $T=430^\circ\text{C}$. The solid line is a best fit of (16b) giving $\Gamma=1.1\pm 0.2\text{ cm}^{-1}$.

has allowed a measurement of the dispersive profile of the resonance suitable to a quantitative interpretation. A comparison of the measured profile with the predictions of a theoretical model using independently determined atomic parameters, has shown a clear evidence of a line-broadening effect due to cesium resonant collisions. By including a collisional contribution to the damping rate of the atomic coherences, the theoretical and experimental line shapes are in excellent agreement.

ACKNOWLEDGMENTS

The research has been carried out at the European Laboratory for Non-Linear Spectroscopy (LENL). J.Z. and P.L. acknowledge the support of the National Science Foundation. S.C. and M.M. wish to thank Professor E. Arimondo for helpful discussions.

- [1] U. Fano, *Phys. Rev.* **124**, 1866 (1961).
- [2] G. Alzetta, A. Gozzini, L. Moi, and G. Orriols, *Nuovo Cimento B* **36**, 5 (1976).
- [3] K. J. Boller, A. Imamoglu, and S. E. Harris, *Phys. Rev. Lett.* **66**, 2593 (1991).
- [4] P. E. Coleman and P. L. Knight, *J. Phys. B* **15**, L235 (1957).
- [5] M. V. Fedorov and A. M. Movsesian, *J. Opt. Soc. Am. B* **6**, 928 (1989).
- [6] Yu. I. Heller and A. K. Popov, *Opt. Commun.* **18**, 449 (1976).
- [7] Yu. Heller, V. F. Lukinykh, A. K. Popov, and V. V. Slabko, *Phys. Lett.* **82A**, 4 (1981).
- [8] P. F. Liao and G. C. Bjorklund, *Phys. Rev. A* **15**, 2009 (1977).
- [9] P. L. Knight, M. A. Lauder, and B. J. Dalton, *Phys. Rep.* **190**, 1 (1990), and references therein.
- [10] L. I. Pavlov, S. S. Dimov, D. I. Metchkov, G. M. Mileva, K. V. Stamenov, and G. B. Altschuller, *Phys. Lett.* **89A**, 441 (1982).
- [11] P. B. Chapple, Ph.D. thesis, Australian National University, Canberra, 1988 (unpublished).
- [12] Jian Zhang and P. Lambropoulos, *Phys. Rev. A* **45**, 489 (1992).
- [13] M. H. R. Hutchinson and K. M. M. Ness, *Phys. Rev. Lett.* **60**, 105 (1988).
- [14] X. Tang, Anne L'Huillier, and P. Lambropoulos, *Phys. Rev. Lett.* **62**, 111 (1989).
- [15] Y. L. Shao, D. Charalambidis, C. Fotakis, J. Zhang, and P. Lambropoulos, *Phys. Rev. Lett.* **67**, 3669 (1991).
- [16] S. Cavalieri, F. S. Pavone, and M. Matera, *Phys. Rev. Lett.* **67**, 3673 (1991).
- [17] D. Feldmann, G. Otto, D. Petring, and K. H. Welge, *J. Phys. B* **19**, 269 (1986).
- [18] J. Fox, *Math. Phys.* **13**, 1196 (1972).
- [19] G. S. Agarwal, *Phys. Rev. A* **18**, 1490 (1978).
- [20] Bo-nian Dai and P. Lambropoulos, *Phys. Rev. A* **36**, 5205 (1987).
- [21] G. V. Marr and D. M. Creek, *Proc. R. Soc. London Ser. A* **304**, 233 (1968).